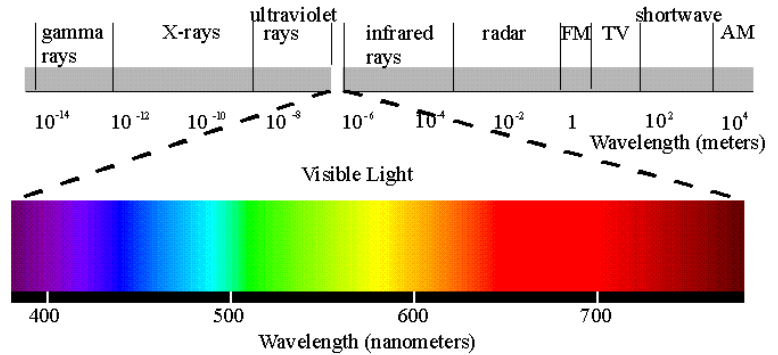


Propriedades ópticas do tecido biológico

Óptica – “luz”

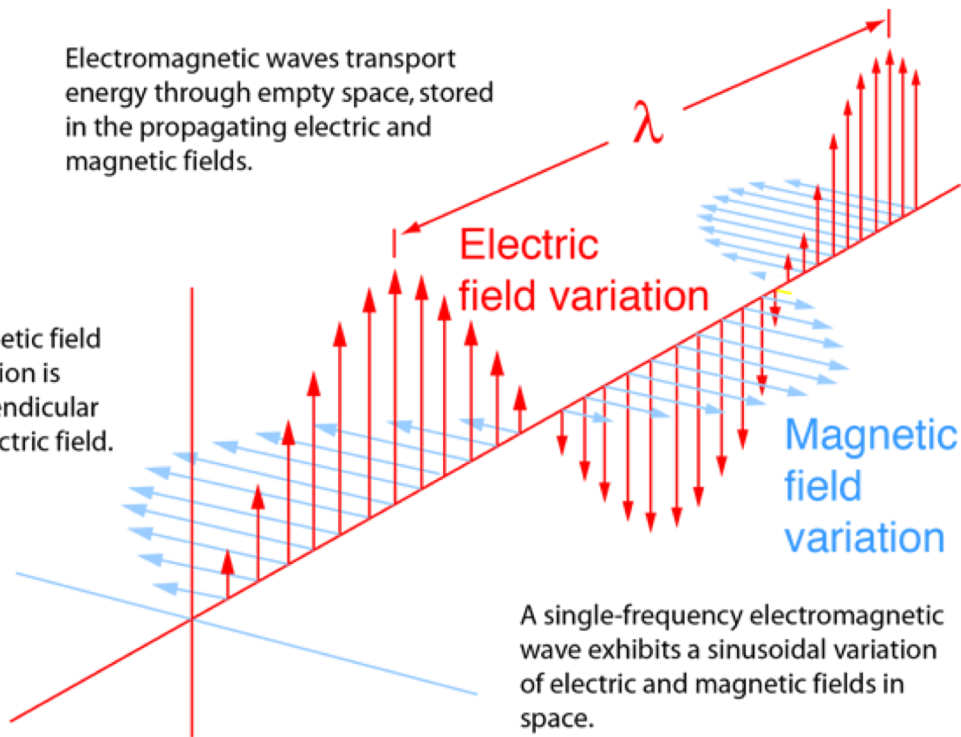
- Óptica – região entre 100 nm a 1 μm .
- Propagação da luz no tecido
 - Modelo clássico: definição matemática da dinâmica do transporte da luz (cálculo de seção de choque de espalhamento, absorção...)
 - Modelo quântico: conceito do “pacote de energia” (fótons) – processos de transição molecular (absorção, luminescência, espalhamento Raman...)

Onda eletromagnética



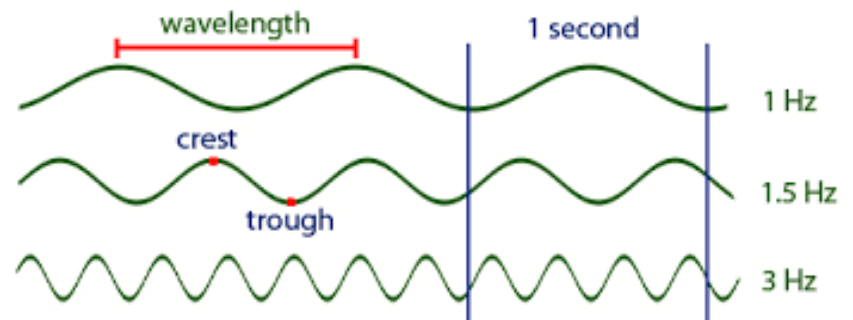
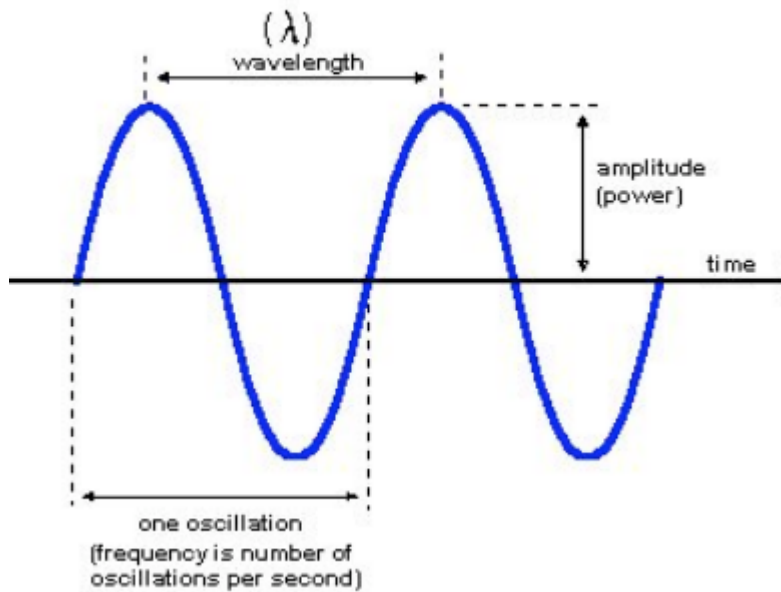
Electromagnetic waves transport energy through empty space, stored in the propagating electric and magnetic fields.

Magnetic field variation is perpendicular to electric field.



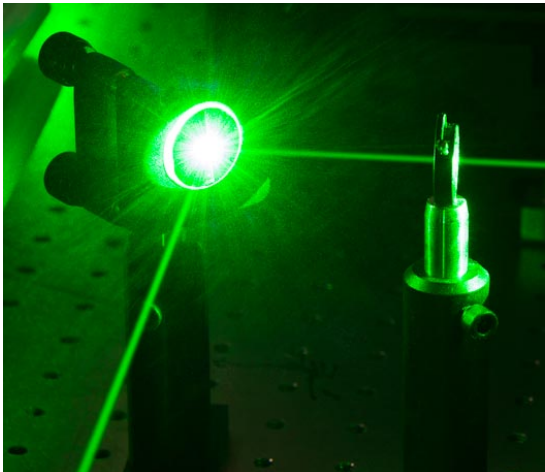
A single-frequency electromagnetic wave exhibits a sinusoidal variation of electric and magnetic fields in space.

Comprimento de onda



LASER

- Luz com características especiais



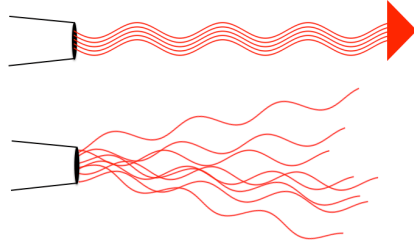
- **Monocromaticidade** (cor única)
- **Coerência** (fótons em fase)
- **Colimação** (ondas praticamente paralelas)



LASER

- Luz com características especiais

Luz laser coerente

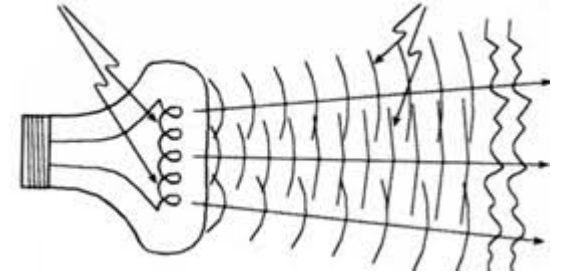


- Monocromaticidade (cor única)
- **Coerência** (fótons em fase)
- Colimação (ondas praticamente paralelas)

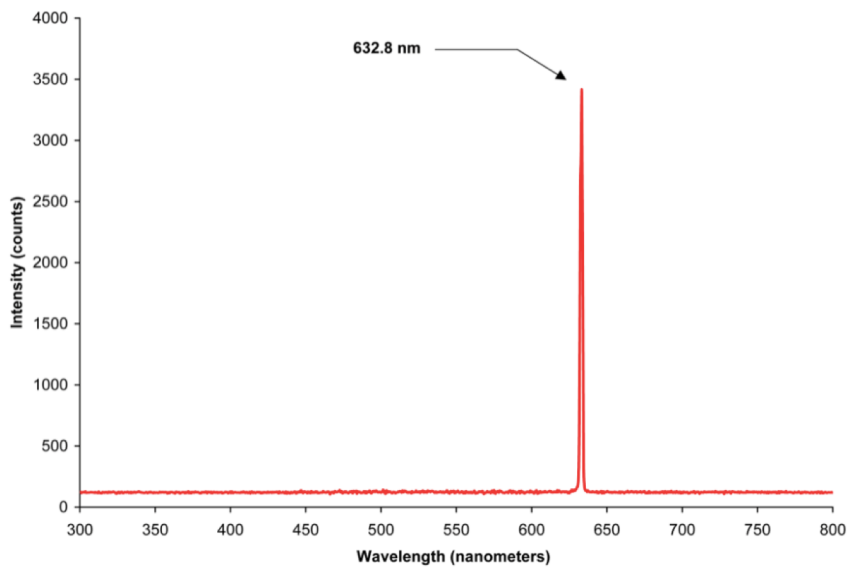
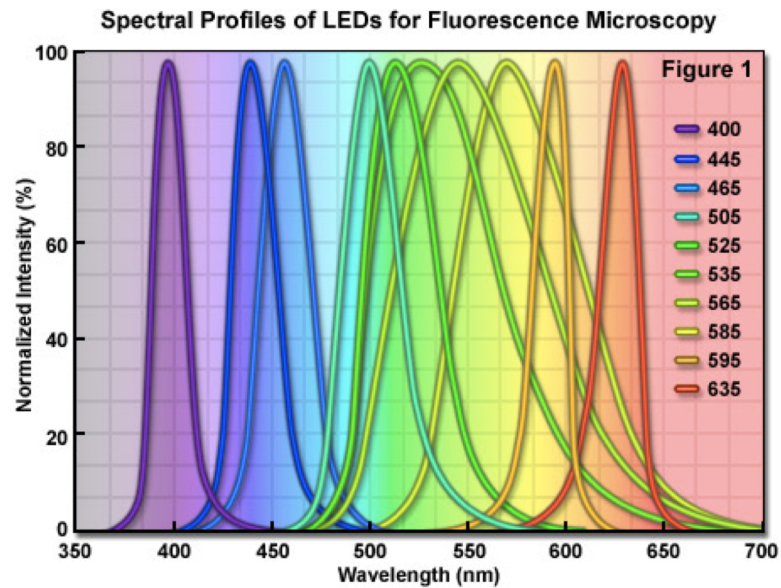
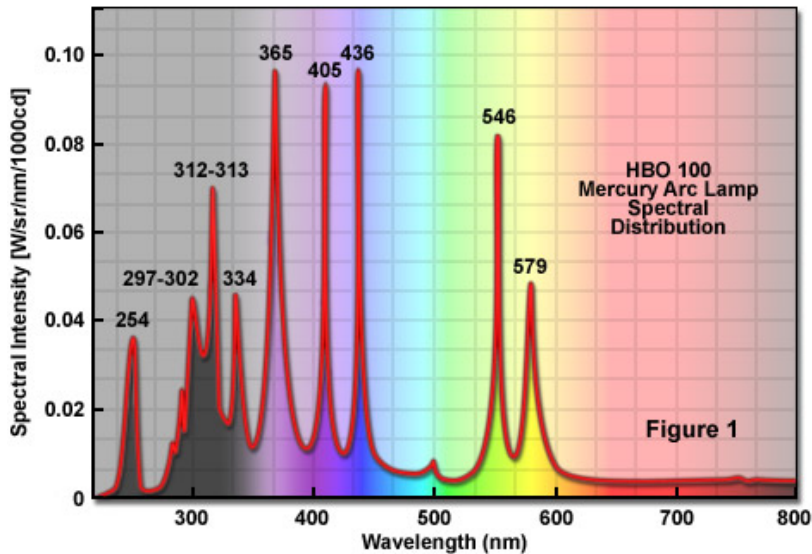
Luz LED não-coerente

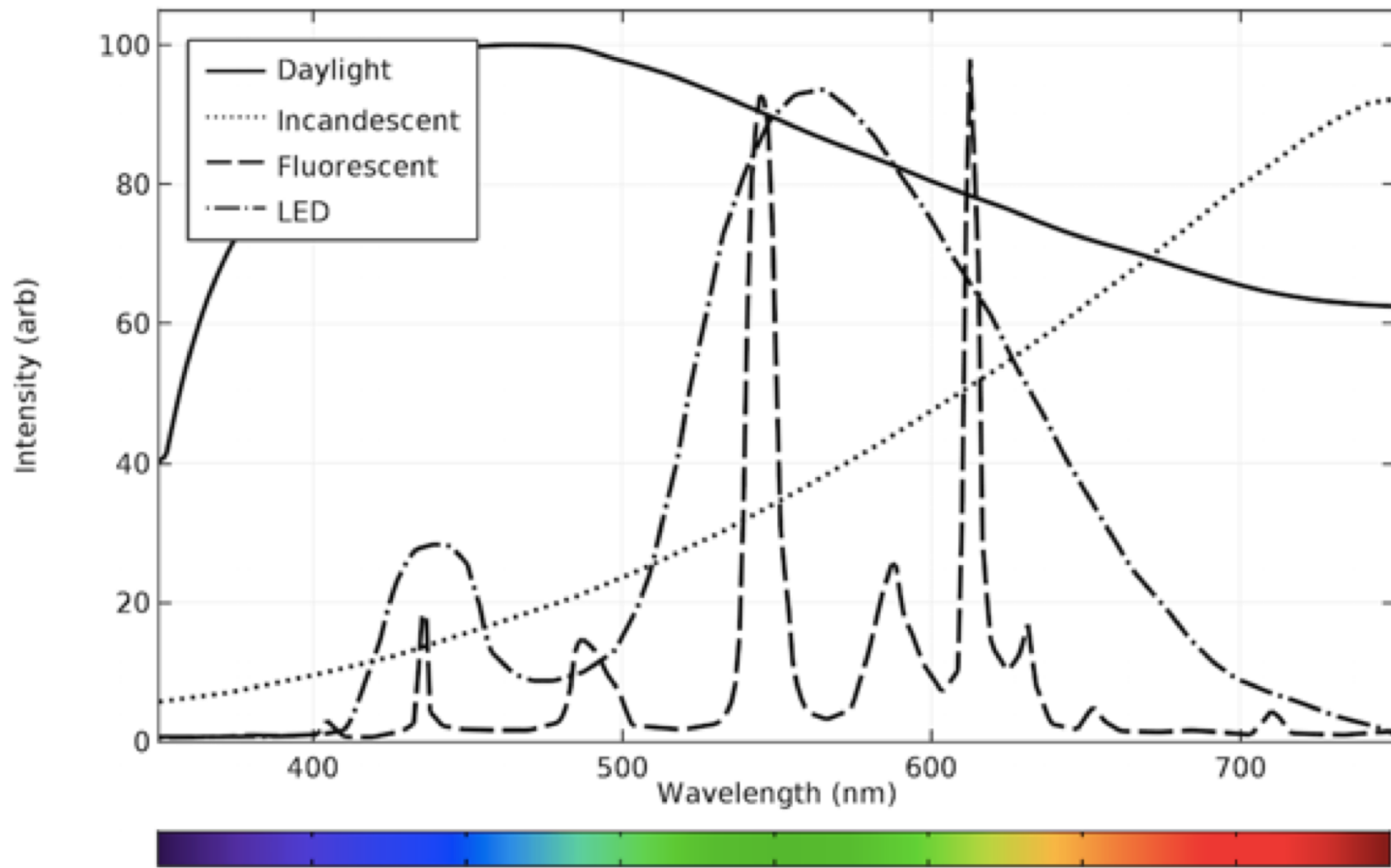


Lâmpada

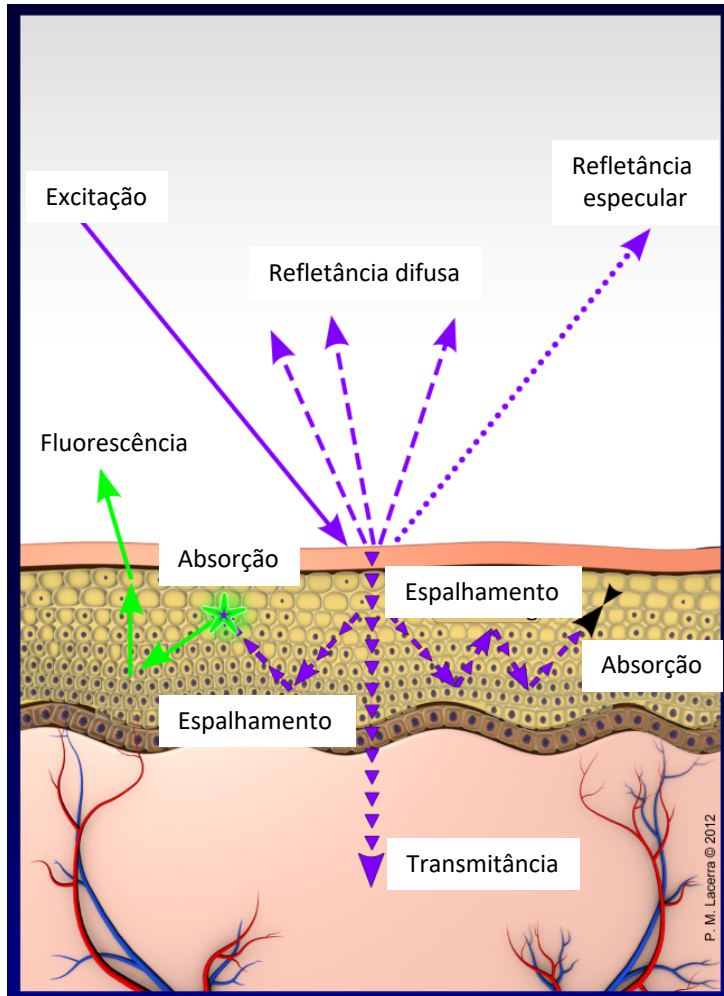


Emissão espectral

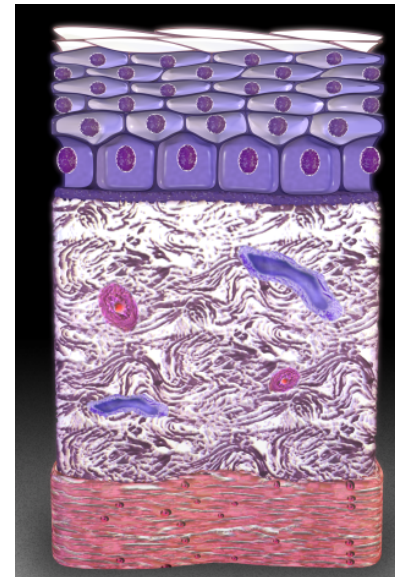




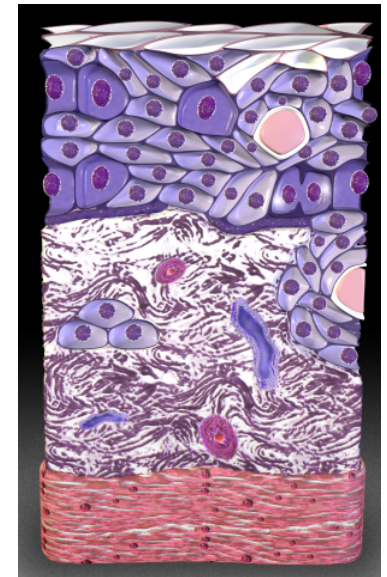
Fótons viajam e interagem com as biomoléculas do tecido



Pele normal



Carcinoma

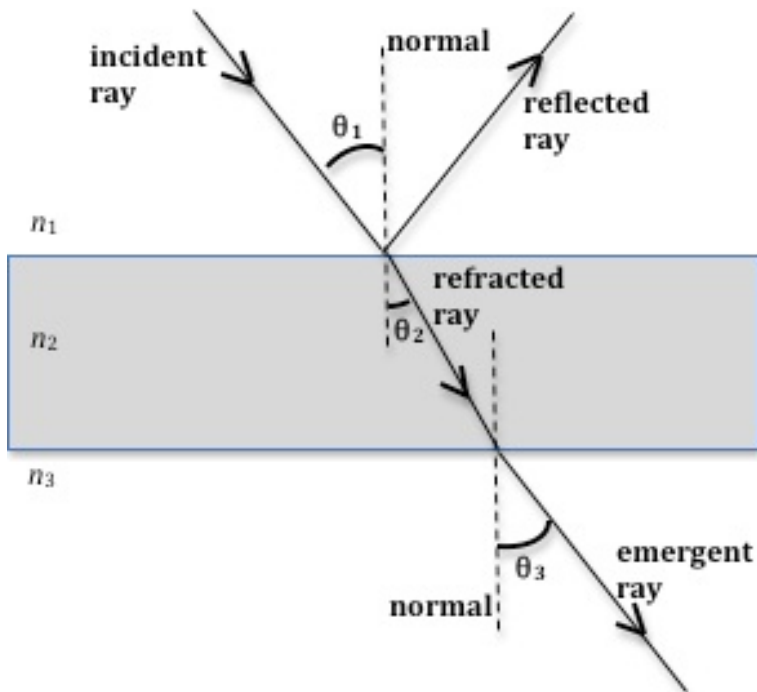


Propagação da luz em tecido biológico

- Espalhamento
- Absorção
- Transmissão

Refração

- Índice de refração: descreve as propriedades ópticas lineares



$$\sin \theta_2 = \frac{n_1}{n_2} \sin \theta_1$$

$$T = \frac{4n_1n_2}{(n_1 + n_2)^2}$$

$$R = 1 - T = \frac{(n_1 - n_2)^2}{(n_1 + n_2)^2}$$

Reflexão Fresnel

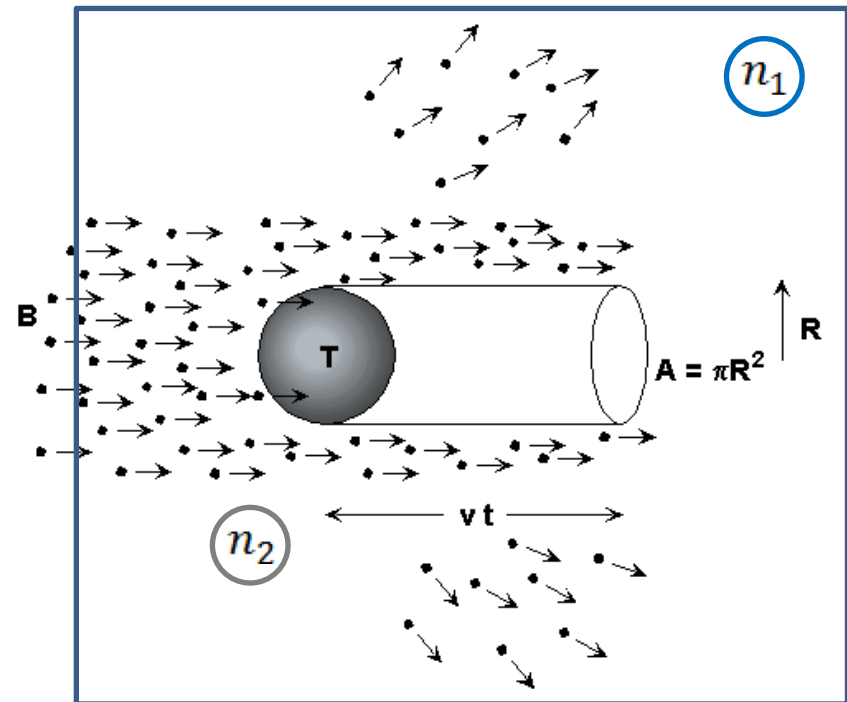


Espalhamento

- Fótons “viajando” dentro do tecido: inclusões com diferentes n

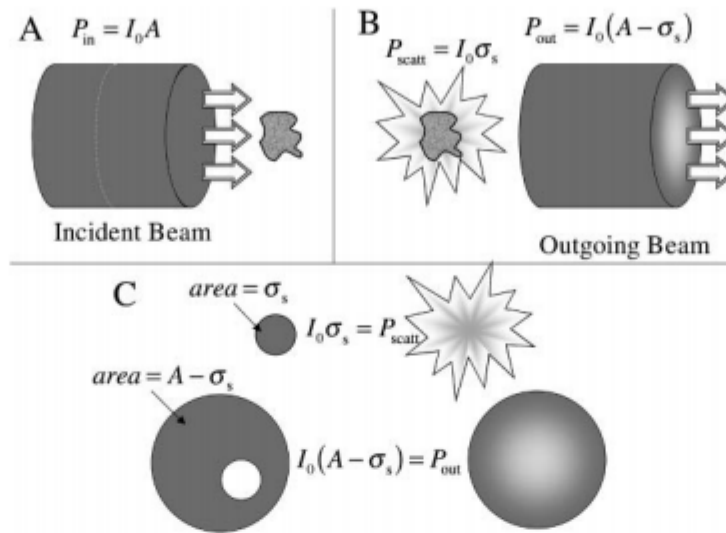
Parte de I_0 é redirecionada em um intervalo de ângulos relativos à partícula espalhadora

Espalhamento depende do tamanho, morfologia e estrutura dos componentes teciduais.



Seção de choque de espalhamento

- Expressa a proporcionalidade entre I_0 e a quantidade de potência espalhada pelo centro espalhador.

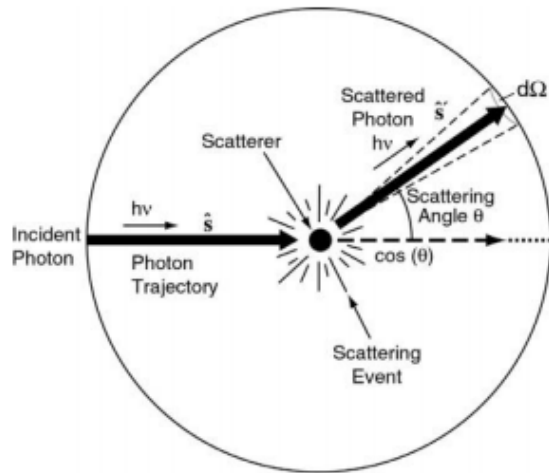


$$\sigma_s(\hat{s}) = \frac{P_{scatt}}{I_0}$$

(direção de propagação da onda plana relativa ao espalhador)

Luz incidente: onda plana (amplitude uniforme em qualquer plano perpendicular à direção de propagação, de pelo menos 1 ordem de grandeza maior que a partícula espalhadora).

Espalhamento



$$\frac{d\sigma_s}{d\Omega}(\hat{s}, \hat{s}')$$

Onde \hat{s}' define o eixo do cone de ângulo sólido $d\Omega$ originado do espalhador.

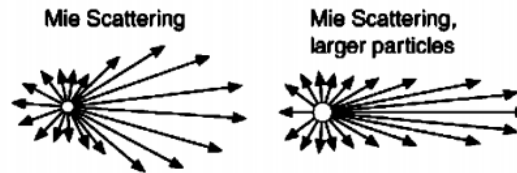
FIGURE 2.6 The differential scattering cross section expresses the angular distribution of the scattered light relative to the incident light. The incident photon travels along the direction \hat{s} and the scattered photon exits in the \hat{s}' direction.

Scattering Regimes

- $< \lambda$ Rayleigh Regime
- E.g. particles in the sky
 - Strongly wavelength dependent
 - Mostly isotropic

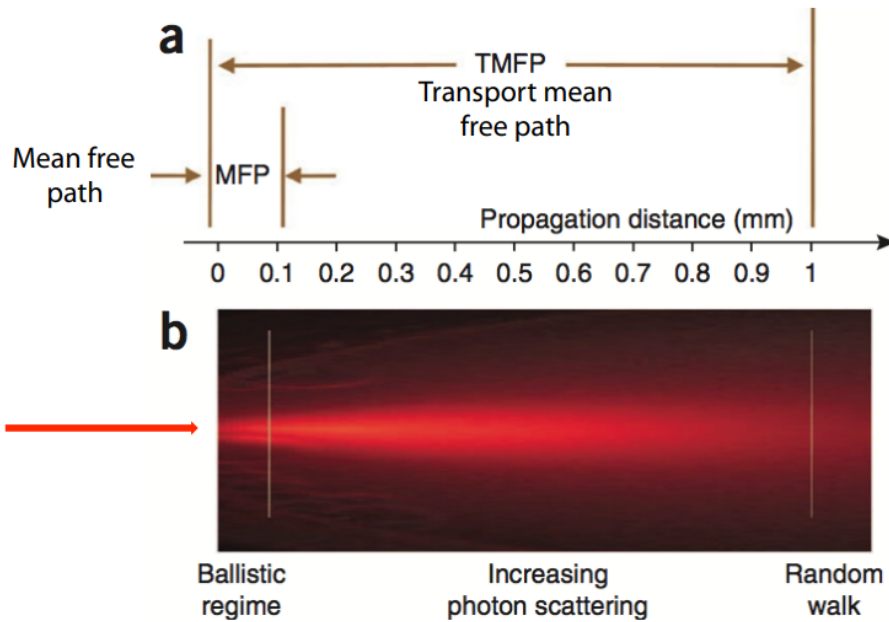


- $\geq \lambda$ Mie Regime
- Cells, water droplets (fog)
 - Anisotropic: mostly forward scattering



$$g = \begin{cases} -1 \dots 0 & \text{Backward scattering (anisotropic)} \\ 0 & \text{Unidirectional scattering (isotropic)} \\ 0 \dots 1 & \text{Forward scattering (anisotropic)} \end{cases}$$

g for most biological tissues: ~ 0.9
(highly forward scattering)



Ntziachristos (2010)

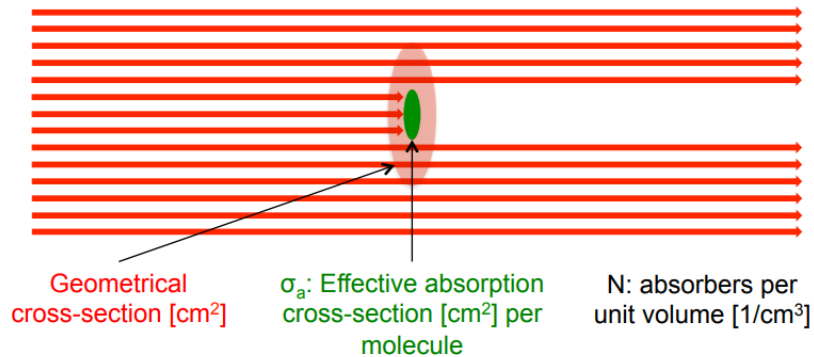
Mean free path: $\frac{1}{\mu_s}$

Transport mean free path: $\frac{1}{\mu_s \cdot (1 - g)}$

- The scattering mean free path is the average distance between scattering events (in biological tissues around 100 μm)
- The transport mean free path can be thought of as the mean distance after which a photon's direction becomes random (in biological tissues around 1 mm)

Absorção

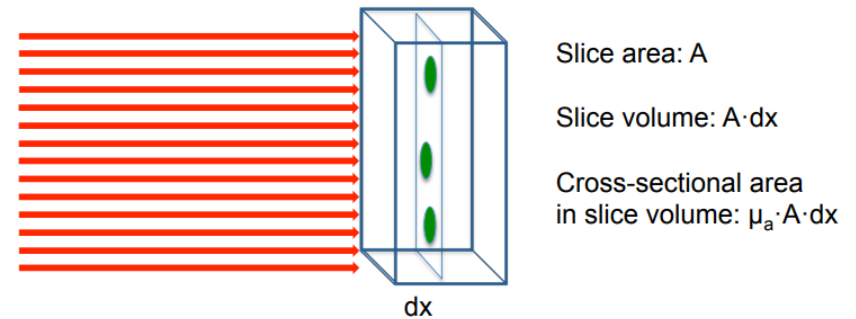
Coeficiente de absorção



$$\mu_a = \sigma_a \cdot N$$

The absorption coefficient μ_a is the total absorption cross-sectional area per unit volume [cm^2/cm^3]

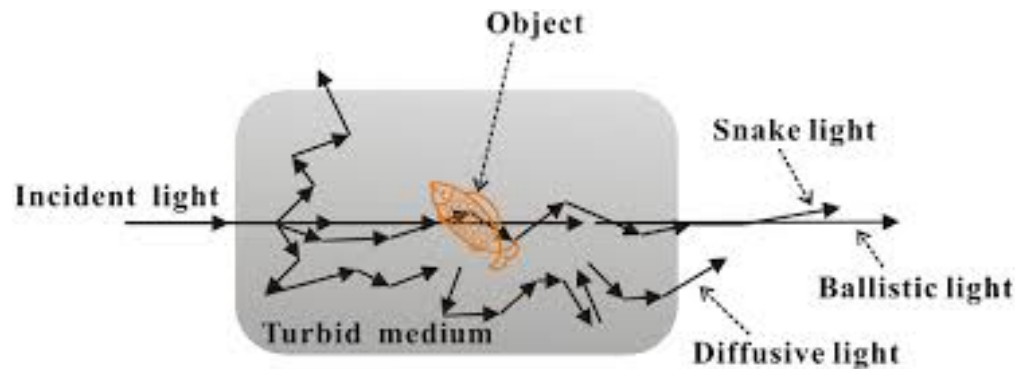
Lei de Beer-Lambert



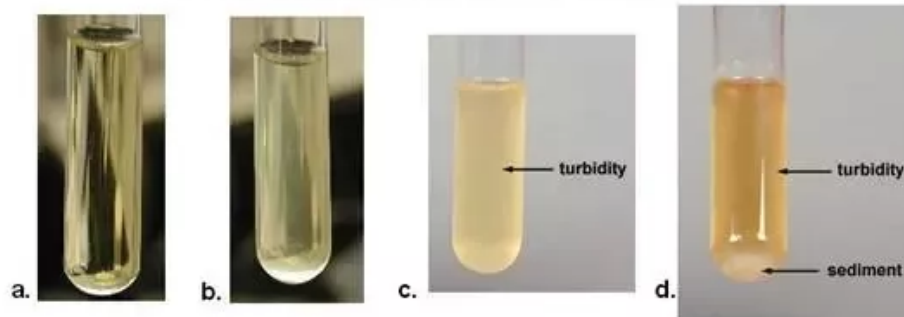
The relative change in intensity equals the total absorption cross-sectional area in the slice divided by the slice area:

$$\frac{-dI}{I} = \frac{\mu_a \cdot A \cdot dx}{A} = \mu_a \cdot dx \Rightarrow I = I_0 e^{-\mu_a x}$$

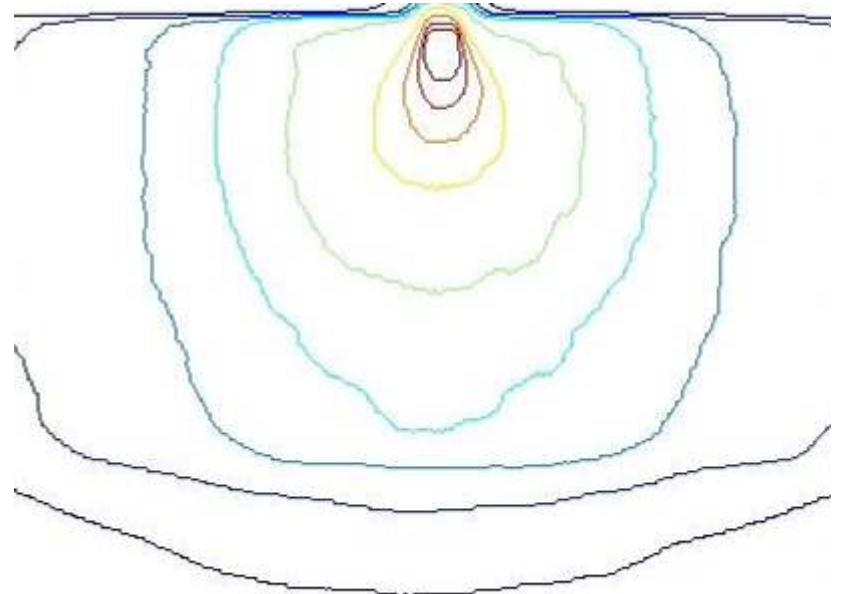
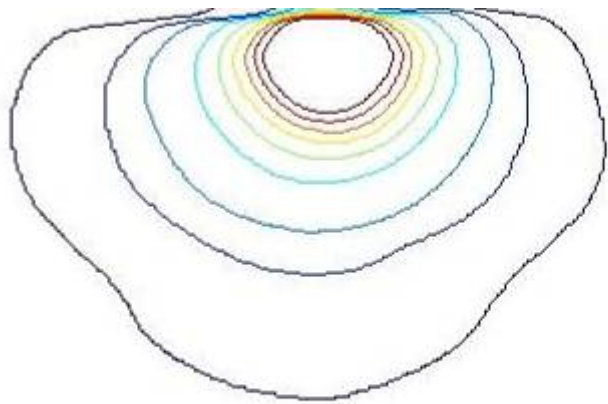
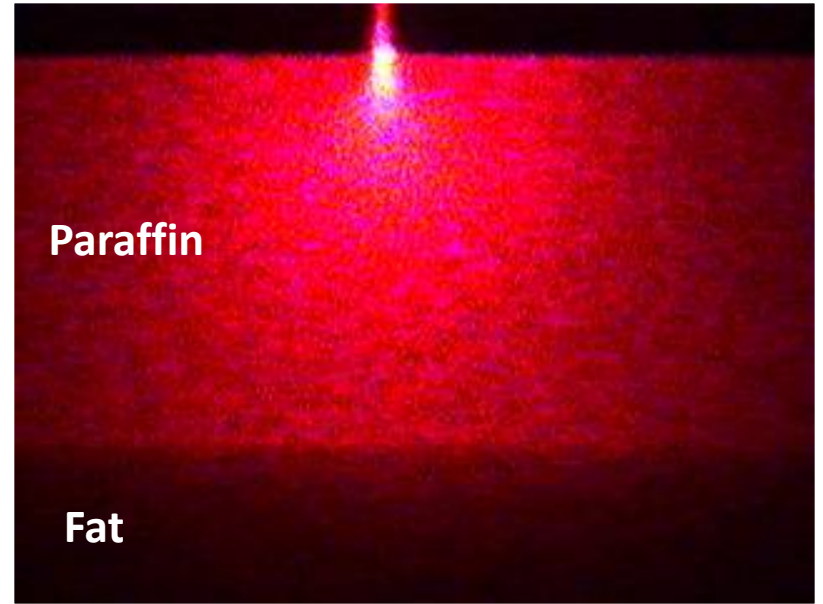
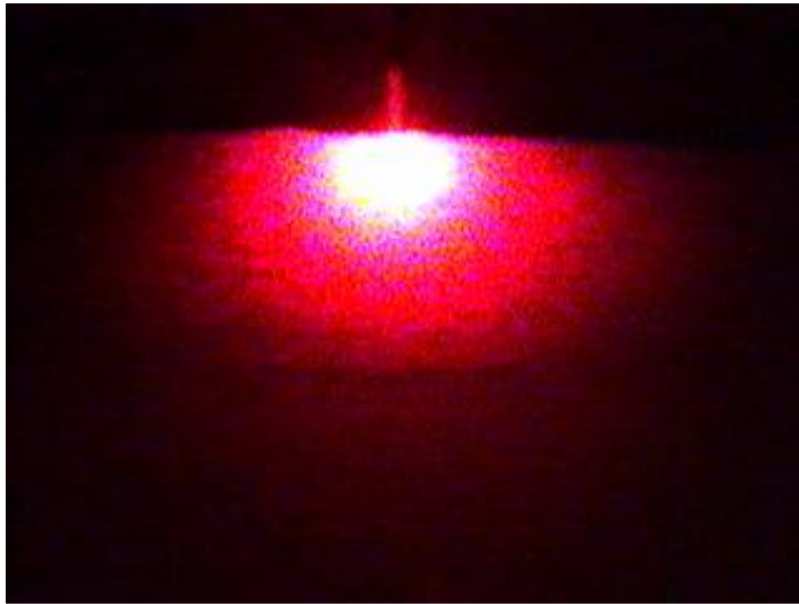
Meios túrbidos



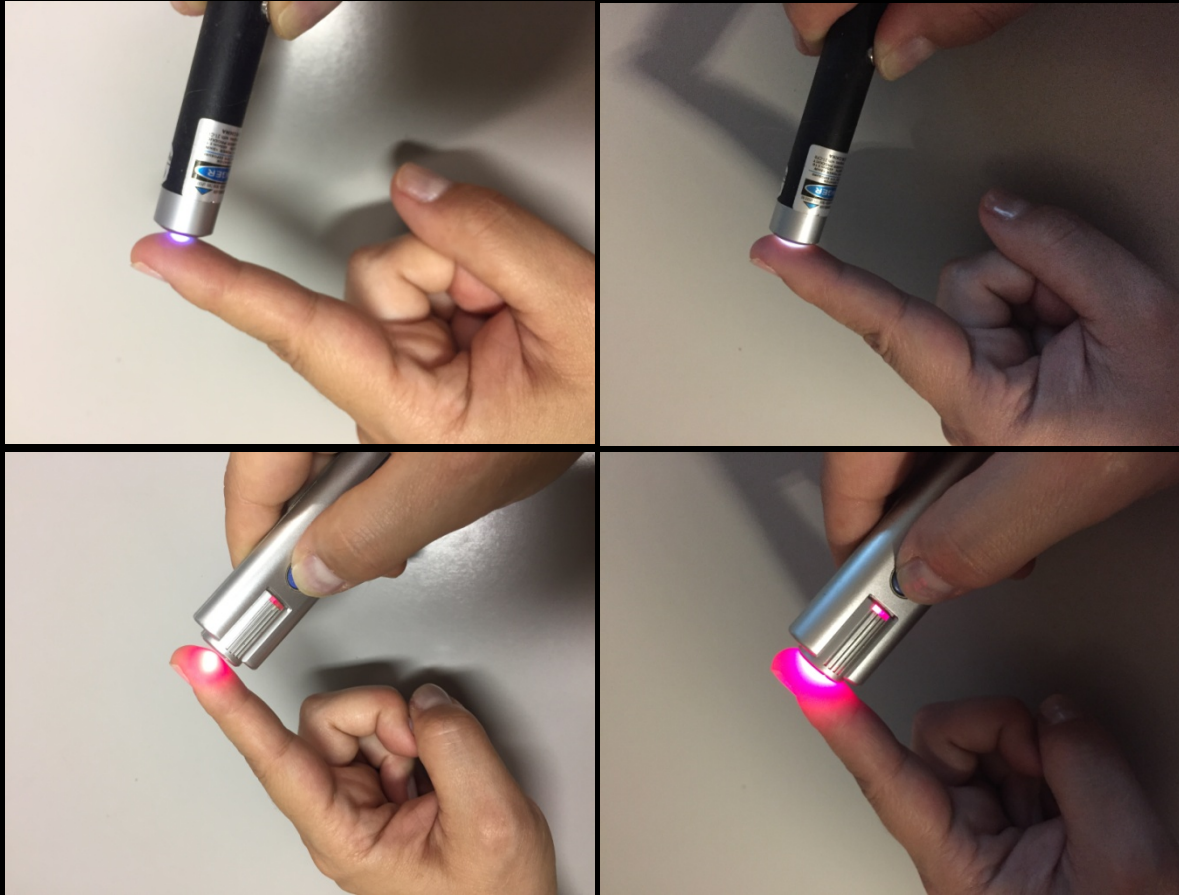
Bacterial Cultures in Broth Media



- Sterile (uninoculated broth) - note how clear the media is
- Broth showing slight turbidity (some bacterial growth)
- Broth showing significant turbidity (a lot of bacterial growth)
- Broth that hasn't been agitated (shaken)



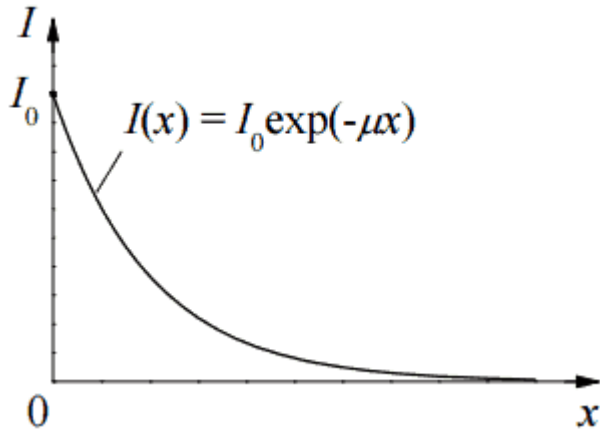
Cor x propagação



Cor x propagação



Atenuação da luz – profundidade de penetração em tecidos biológicos



$$I = I_0 e^{-\mu x}$$

Where:

I = the intensity of photons transmitted across some distance **x**

I₀ = the initial intensity of photons

s = a proportionality constant that reflects the total probability of a photon being scattered or absorbed

μ = the linear attenuation coefficient

x = distance traveled

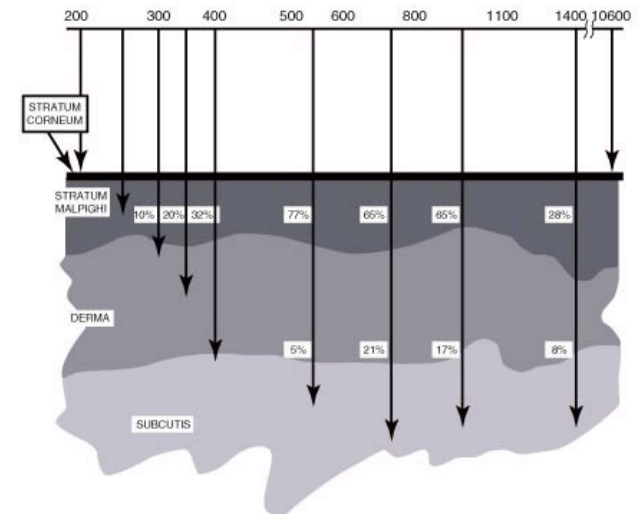
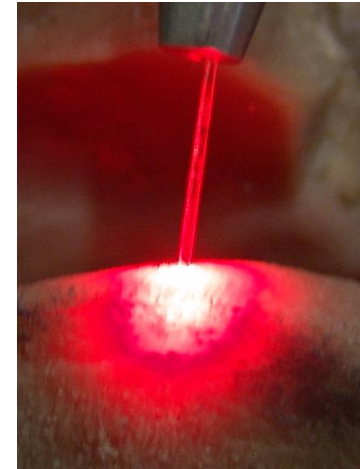


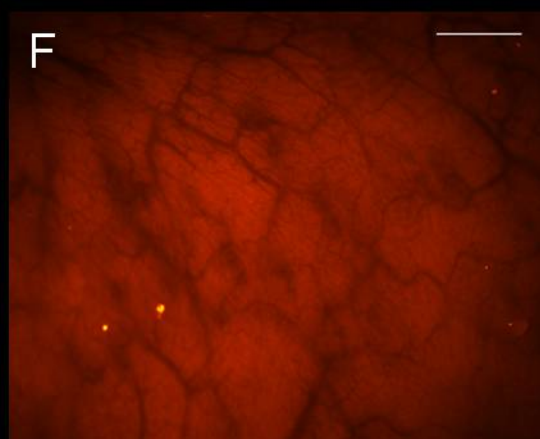
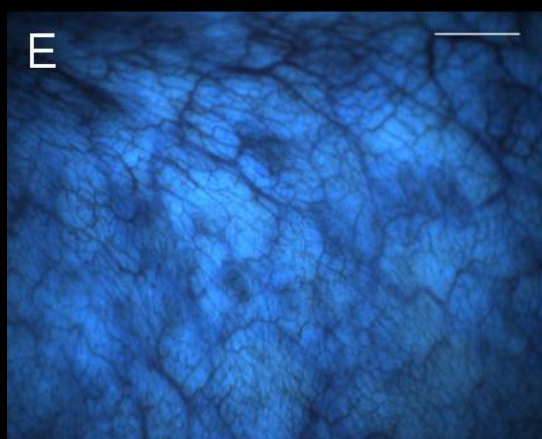
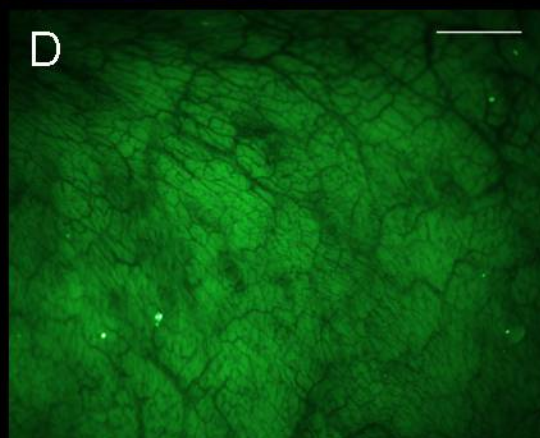
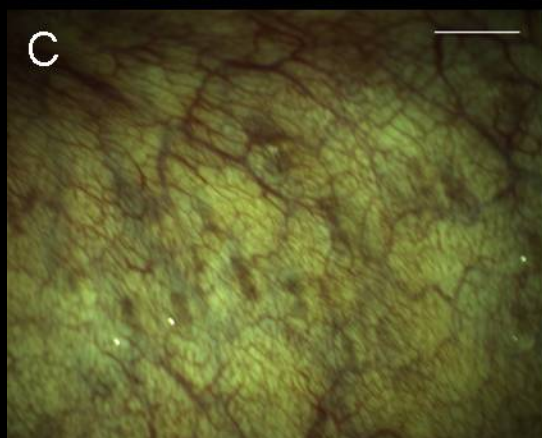
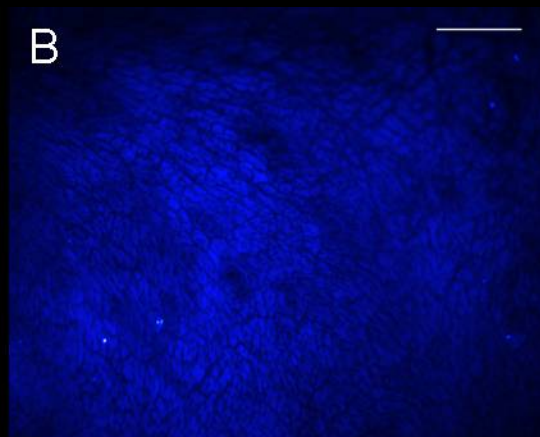
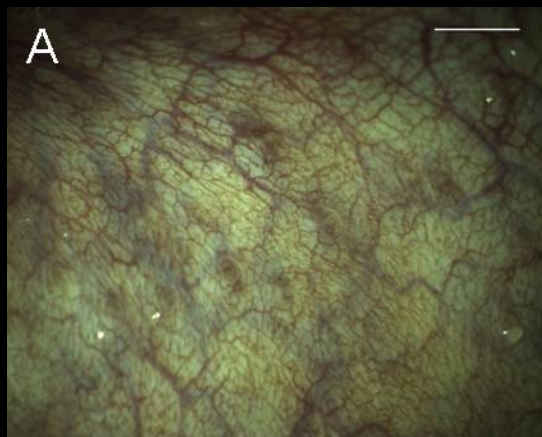
Table 1

In vivo optical properties at commonly used treatment wavelengths for PDT

Tissue	λ (nm)	μ_a (cm ⁻¹)	μ_s' (cm ⁻¹)	Experimental Method	References	
Bladder	532	0.27–0.71	1.28–3.30	4	[108]	
	630	0.28–0.76	2.5–6.37	4	[108]	
Bone	650	0.09–0.14	12.5–15.8	1	[109]	
	760	0.07–0.09	11.9–14.1	1	[109]	
Brain	420	0.01–3.51	18.75–55.83	4	[108]	
	532	0.02–3.84	0.10–46.3	4	[108]	
	630	0.02–0.50	3.72–21.97	4	[108, 110, 111]	
	760	0.11–0.17	4.0–10.5	1, 2	[6, 112]	
	780	0.078–0.089	8.42–9.16	2	[8]	
Breast	660	0.037–0.110	11.4–13.5	1, 4	[113–118]	
	760	0.031–0.10	8.3–12.0	1, 4	[115, 116, 118–121]	
	900	0.096–0.29	3.33–5.86	1, 4	[9, 115, 118, 122]	
Tumor	530	0.60–0.86	28.0–32.1	4	[123]	
	690	0.070–0.10	14.7–17.3	2	[124]	
	895	0.068–0.102	12.4–13.1	2	[124]	
Bowel	Small	630	0.19–0.21	8.95–10.05	4	[35, 76]
	Large	630	0.12–0.18	10.11–10.42	4	[35, 76]
Diaphragm	661	0.15–1.08	9.65–21.7	4	[125]	
Heart	630	0.03–1.55	17.56–75.06	4	[126]	
	661	0.12–0.18	5.22–90.80	4	[125]	

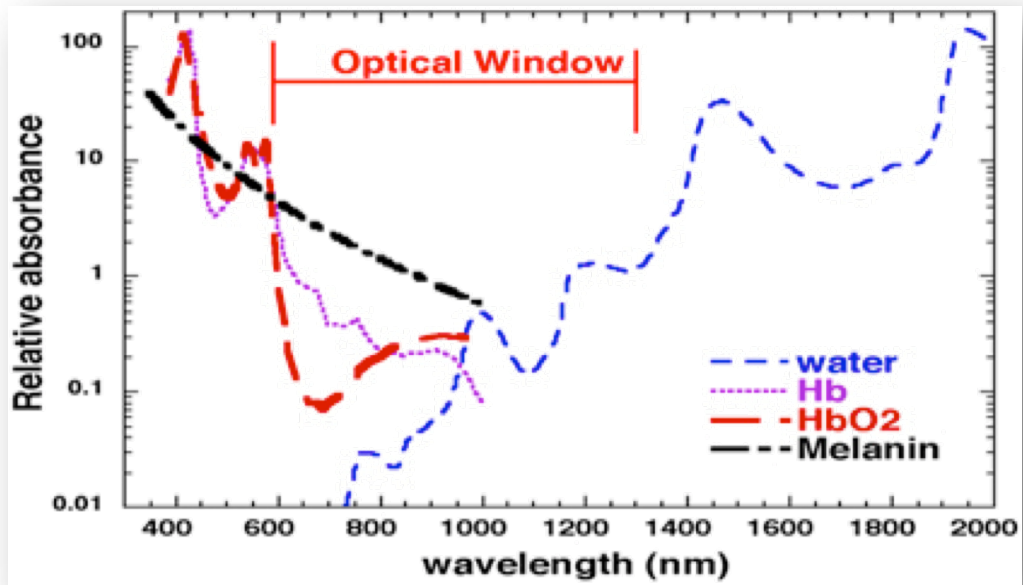
Liver	630	1.15–1.56	21.6–30.4	4	[35, 76]
Lung	630	0.16–1.36	1.07–83.81	4	[126]
	661	0.49–0.88	21.14–22.52	4	[125]
Pericardium	630	0.13–0.33	13.0–21.9	4	[35, 76]
Prostate	630	0.05–1.0	3.41–17.02	4	[127, 128]
	650	0.14–0.61	5.24–22.68	4	[128–130]
	672	0.09–0.72	7.1–25.0	1, 3	[44, 128, 129, 131]
	732	0.09–0.72	3.37–29.8	3	[39, 129, 131]
	762	0.11–1.6	1.2–40.0	2, 3	[11, 129, 131–133]
Skin	630	0.05–1.11	2.26–20.95	1, 4	[34, 35, 126, 134, 135]
	661	0.51–0.64	2.24–5.77	4	[116, 125, 136]
	800	0.16–0.23	6.80–9.84	1	[116, 137, 138]

[Open in a separate window](#)¹Time of flight absorption spectroscopy²Frequency Resolved Spectroscopy³CW Absorption Transmittance Spectroscopy⁴CW Absorption Reflectance Spectroscopy



Star Trek - Tricorder





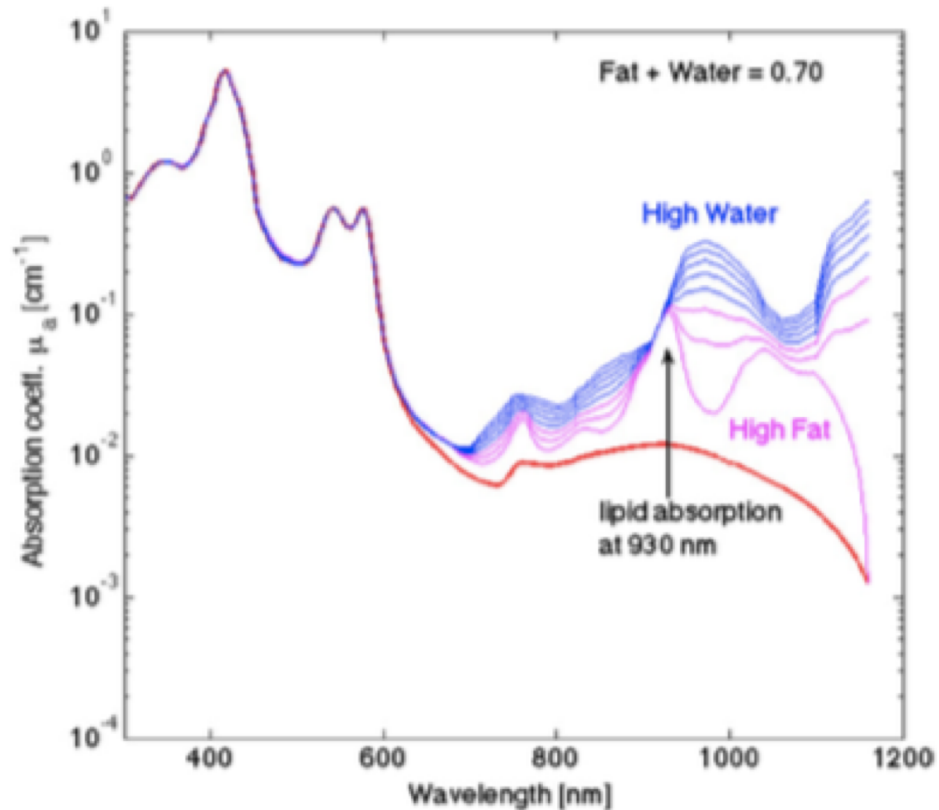
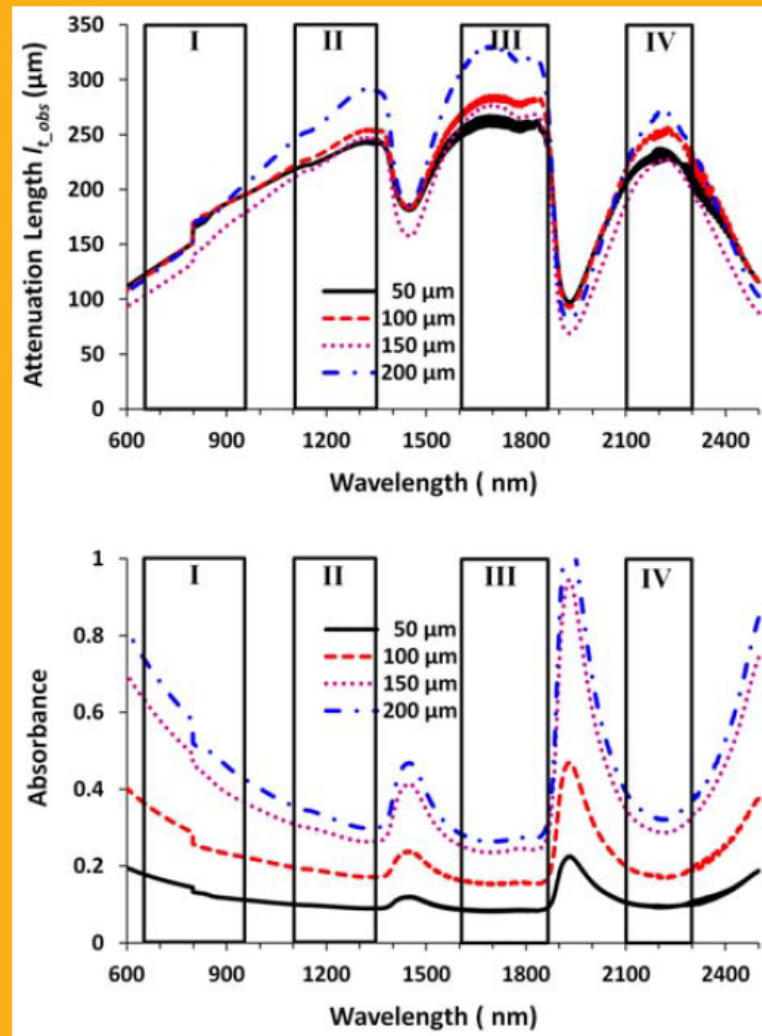


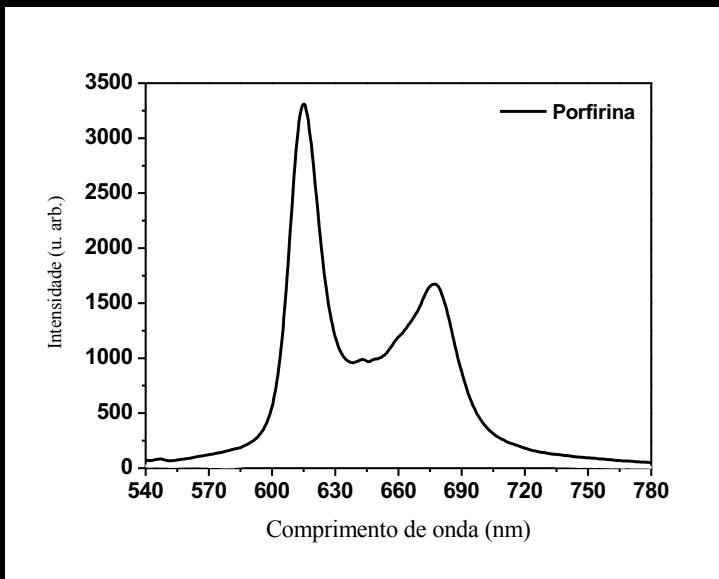
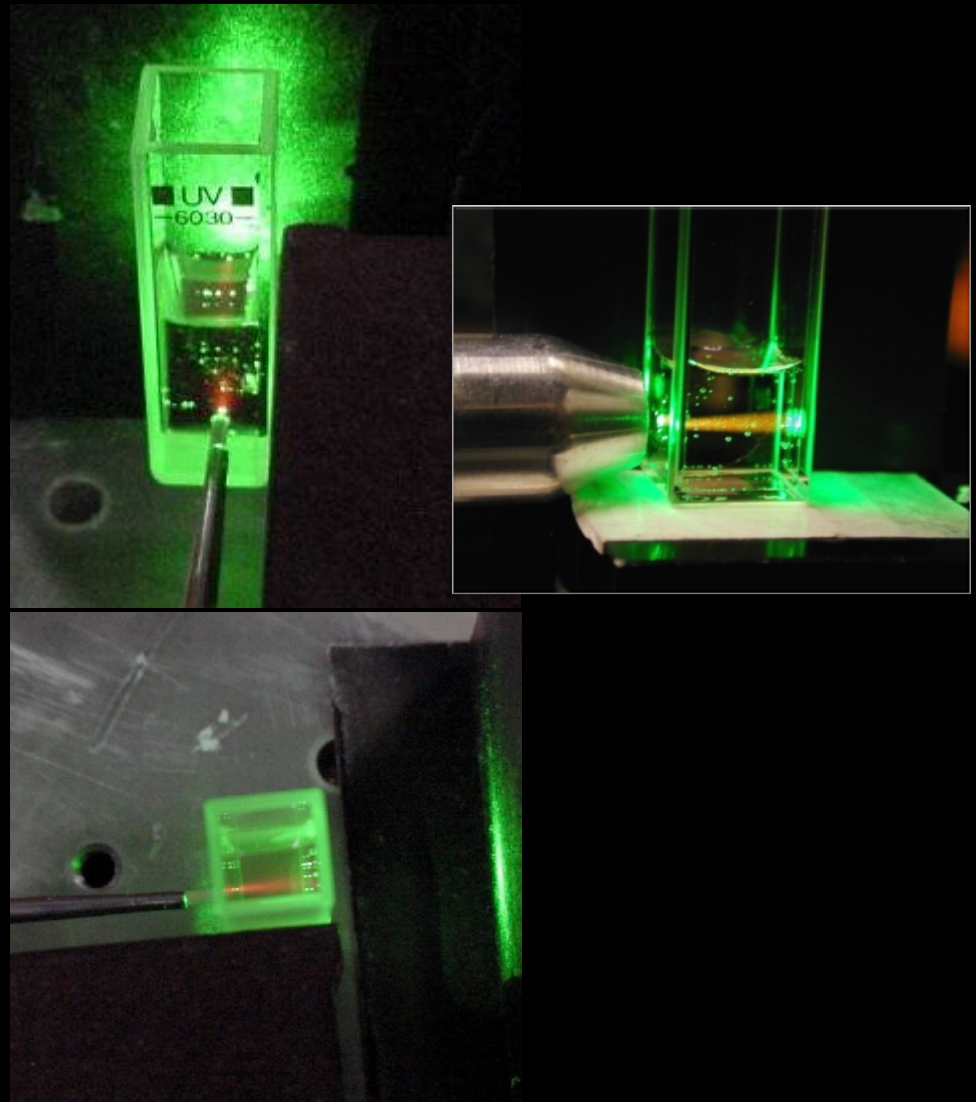
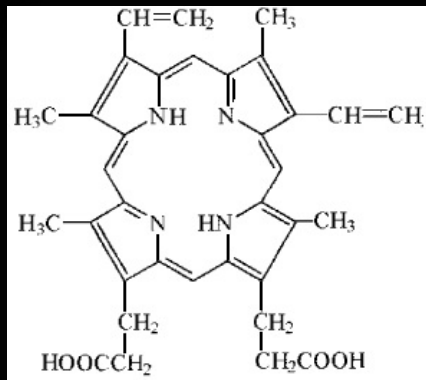
Figure 16. The absorption spectrum of a tissue ($B = 0.002$, $S = 0.75$, $f_{v,\text{fibrous}} = 0.30$) that varies its water content from 0 by 0.1 to 0.7 as the fat content varies from 0.7 by 0.1 to 0, such that fat + water = 0.7. Magenta lines are for high fat, low water, and the fat signature is clearly present at 930 nm (arrow). The blue lines are for low fat, high water ($W \geq 0.3$), and the fat signature is less obvious. (Based on the fat spectrum of van Veen *et al* (2004).)

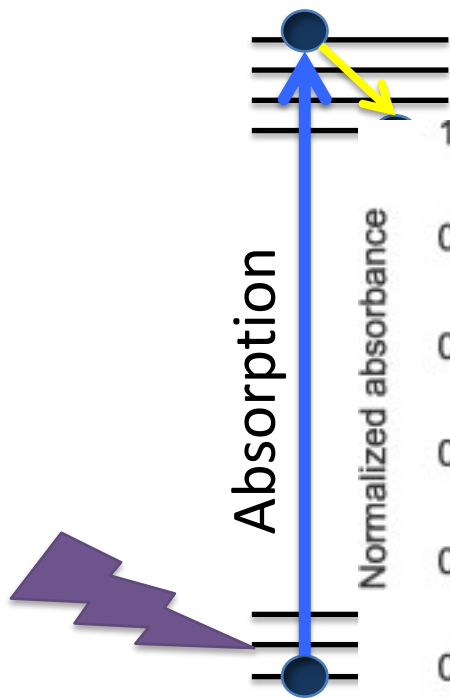
Near-infrared (NIR) radiation has been employed using one- and two-photon excitation of fluorescence imaging at wavelengths 650–950 nm (optical window I) for deep brain imaging; however, longer wavelengths in NIR have been overlooked due to a lack of suitable NIR-low band gap semiconductor imaging detectors and/or femtosecond laser sources. This research introduces three new optical windows in NIR and demonstrates their potential for deep brain tissue imaging. The transmittances are measured in rat brain tissue in the second (II, 1,100–1,350 nm), third (III, 1,600–1,870 nm), and fourth (IV, centered at 2,200 nm) NIR optical tissue windows. The relationship between transmission and tissue thickness is measured and compared with the theory. Due to a reduction in scattering and minimal absorption, window III is shown to be the best for deep brain imaging, and windows II and IV show similar but better potential for deep imaging than window I.



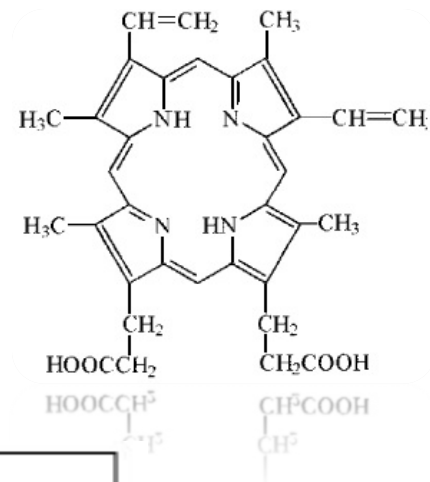
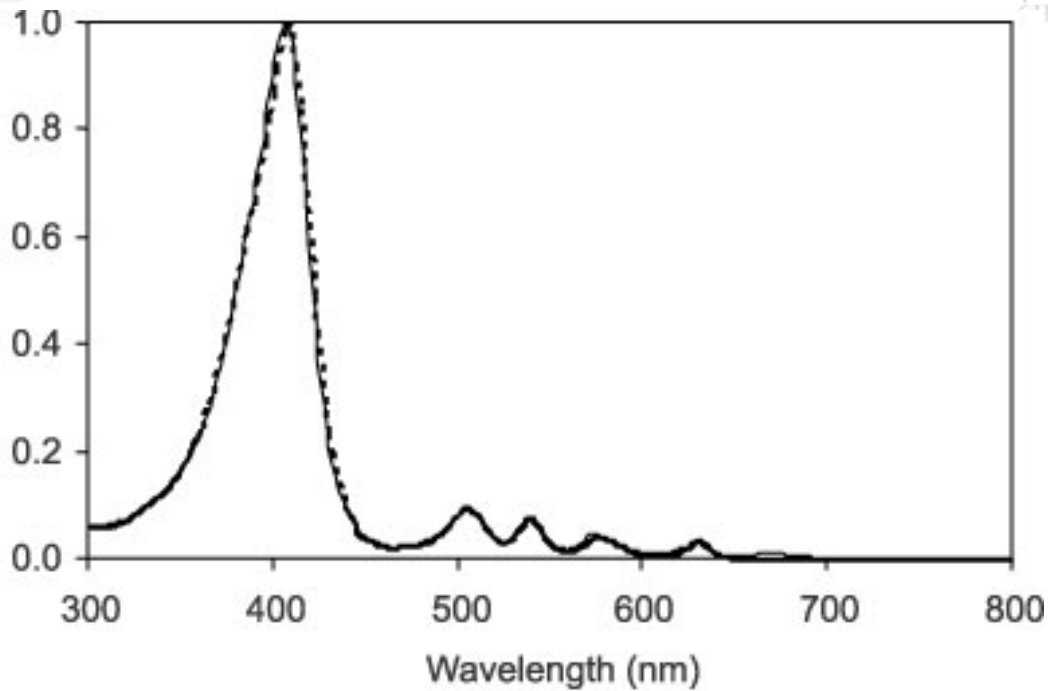
L. Shi et al., J Biophotonics 2015.

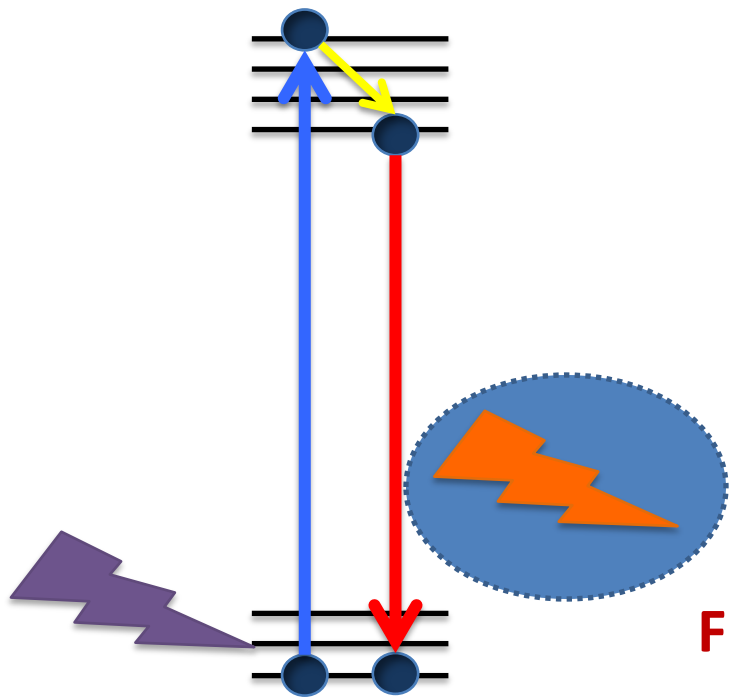
FLUORESCÊNCIA



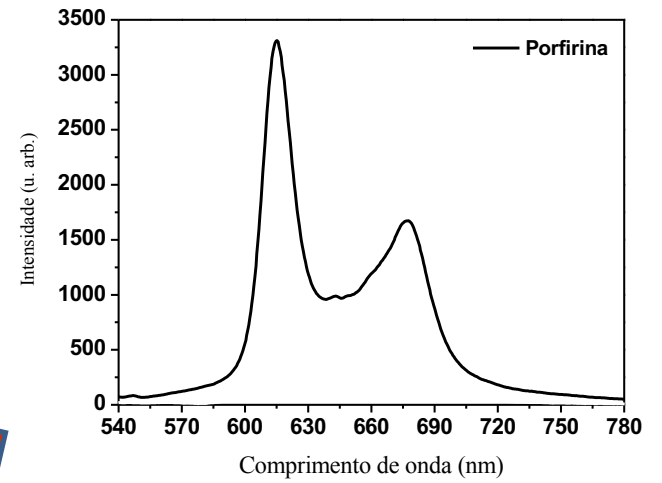
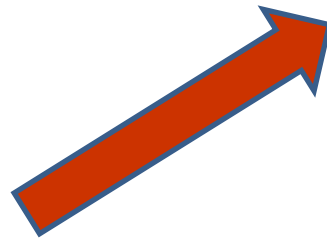


Excited state





Fluorescence



FLUOROPHORES	BIOMOLECULES / CELL LOCALIZATION	EXCITATION Peak position range	EMISSION Peak position range
Aromatic AminoAcid Residues	Proteins A= Phe+Tyr; B= Trp+Phe+Tyr	240 – 280 nm	280 – 350 nm
Collagen Elastin Cytokeratins	Extracellular matrix Connective tissue Epithelia	330 – 340 nm 350, 420 nm 280, 325 nm	400 - 410 nm 420, 510 nm 495, 525 nm
Reduced Pyridine Nucleotides	NAD(P)H (Cofactors in metabolism) mitochondria / cytoplasm	330 – 380 nm	440 nm (bound) 462 nm (free)
Flavins Flavin Nucleotides	Riboflavin, FMN, FAD (Coenzymes of Flavoproteins) mitochondria / cytoplasm	350 – 370 nm 440 – 450 nm	480 – 540 nm
Porphyrins (Zinc- Protoporphyrin)	Prosthetic group of proteins Hemoglobin Myoglobin Cytochrome Erythroid cells	405 nm 500 – 600 nm	630, 670 nm
Lipofuscins Lipopigments	Pigments (cell catabolism / cell age) cytoplasm	UV 400 – 500 nm	> 540 nm
Vitamins	Vitamin A Vitamin B6 & Precursors	370 – 380 nm 290 – 310 nm / 375 – 395 nm	490 – 510 nm 375 – 395 nm / 400 – 500 nm
Lipids	Arachidonic Acid Phospholipids	330, 350 nm 430 - 440 nm	470 – 480 nm 520 – 570 nm
Catecholamines Serotonin	Neurotransmitters	280 – 290 nm 305, 360 (dimer), 420 (trimer) nm	320 – 340 nm 350, 440 (dimer), 520 (trimer) nm

G. Bottiroli and AC. Croce – The autofluorescence spectroscopy of cells and tissues as a tool for biomedical diagnosis. In: *Lasers and current optical techniques in biology*. G. Palumbo and R. Pratesi Eds. Comprehensive Series in Photosciences, vol. 5. The Royal Chemical Society, London. 2004.